

Spatial fine-structure in trapped and precipitating medium-energy electrons in the noon sector.

M.J. Birch⁽¹⁾ & J.K.Hargreaves^(2,1)

(1) Jeremiah Horrocks Institute for Astrophysics,
University of Central Lancashire, UK.

(2) Department of Physics, Lancaster University, UK.

Introduction

It is known that in the noon sector the flux of electrons exceeding 30 keV detected by the vertical counter (measuring the precipitating electron component) on the Polar Orbiting Environmental Satellites (POES) varies non-linearly with the flux detected by the horizontal counter (measuring the trapped component). The purpose of the present study is to explore this relationship in greater detail on the fine (10 km) spatial scale.

Data Selection (1)

- Satellites: POES; sun-synchronous orbits; altitude 850 km.
- Detectors: vertical and horizontal, with 9° offsets; 30° reception cones; vertical detector 17° to magnetic field; horizontal 78° or 102° to field; calibration, 1 count/s = flux of 100 particles/($\text{cm}^2 \cdot \text{s} \cdot \text{sr}$)
- Selection criteria: LT 1130-1330; geographic latitude 68° - 70°N ; longitude 15.79° - 25.79°E (within 1° lat. and 5° long. of Kilpisjärvi); L-value 5.5-6.4.
- Data from 2001, 2004, 2008; solar-max, -mid, -min.; sunspot numbers (80.0-150.0), (17.9-51.0), (0.5-9.3).
- Data at 2s sample interval; typically 18-20 data points per pass; pass duration approx. 35-40 s., covering ≈ 200 km N-S.

Data Selection (2)

- At least 11 data points per pass.
- At least 30 precipitating counts/s at 30 keV throughout each pass, to ensure a reasonable level of activity.
- Passes checked against readings from proton detectors; small contaminations corrected for; passes with higher contamination rejected.
- Above criteria met for 43 passes in all, 10 from 2001, 17 from 2004, and 16 from 2008.

Overview

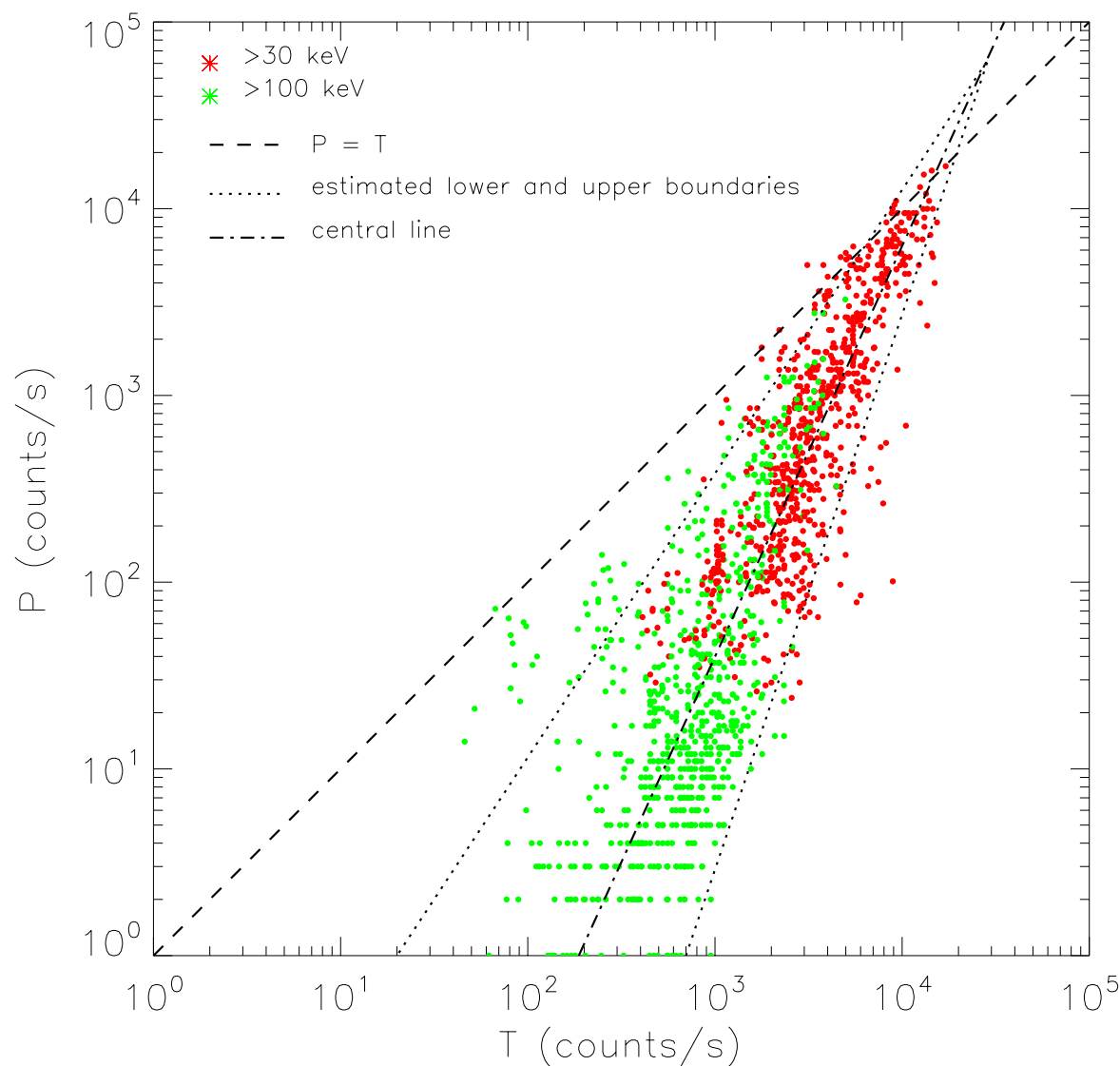


**Figure 1: P and T count rates,
>30 and >100 keV**

- Mass plot of count rates from entire set of 43 passes.
- Includes both >30 and >100 keV data.
- Sharp variation of P with T.
- Not inconsistent with previous observations [1].
- The variability of P is greater at smaller T.
- Central line of plot:
 $P = 10^{-5} \times T^{2.2}$
- Spread, central line to boundary, as a ratio:
 $1.72 \times 10^3 \times T^{-0.725}$

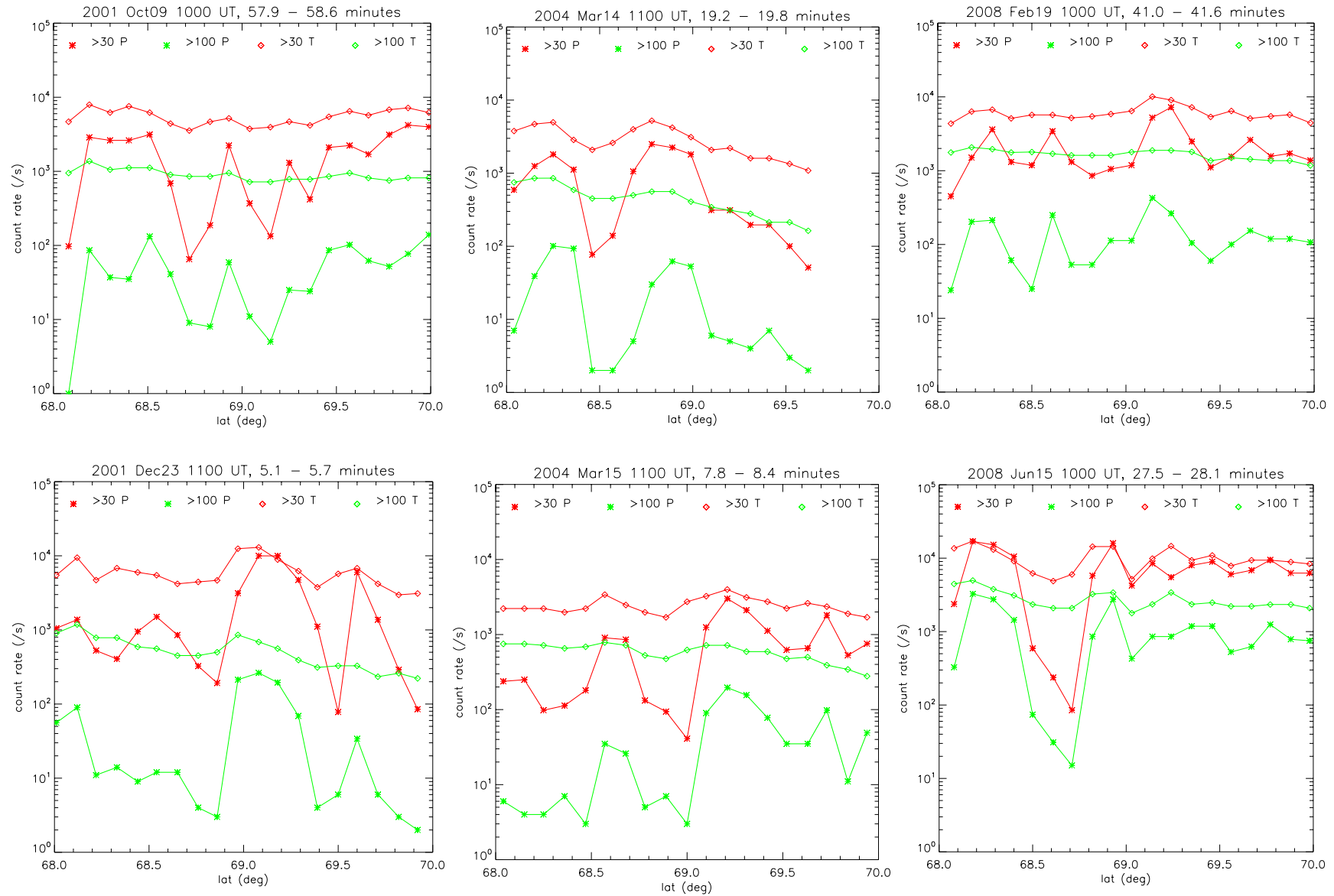
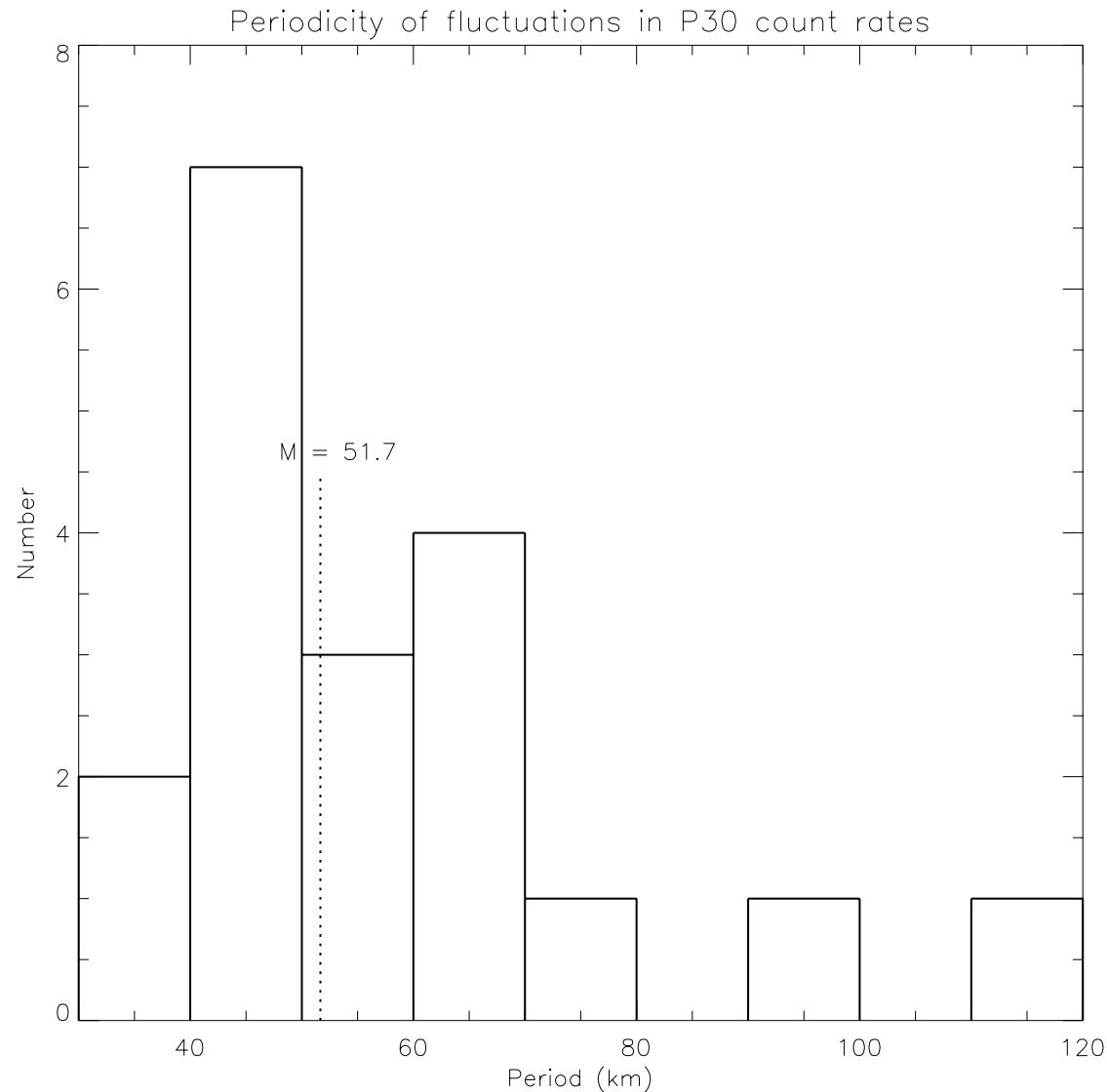


Figure 2: POES count rates for typical passes covering 220 km within 40 secs. The periodicity of the fluctuations is particularly evident in the precipitating flux.



The periodicities have been shown to be spatial rather than temporal [1]. The median value is about 50 km.

The max/min ratio of the fluctuations in this sample of passes ranges from 2 to more than 100 (Figure 2).

Figure 3: Histogram of the periodicities (M = median).

Three types of behaviour

Figure 4 illustrates the behaviour of the precipitating flux (P) as a function of the trapped flux (T). By inspection, three types of behaviour may be identified:

Type A: $P \approx T$.

$P/T \geq 0.7$ was taken as the definition.

Type B: $P \propto T^2$.

These passes were selected from the plots by inspection.

Type C: Substantial variation in P without significant variation in T.

Figure 4(a) illustrates types A and B, Figure 4(b) shows type C, and Figure 4(c) includes all three types.

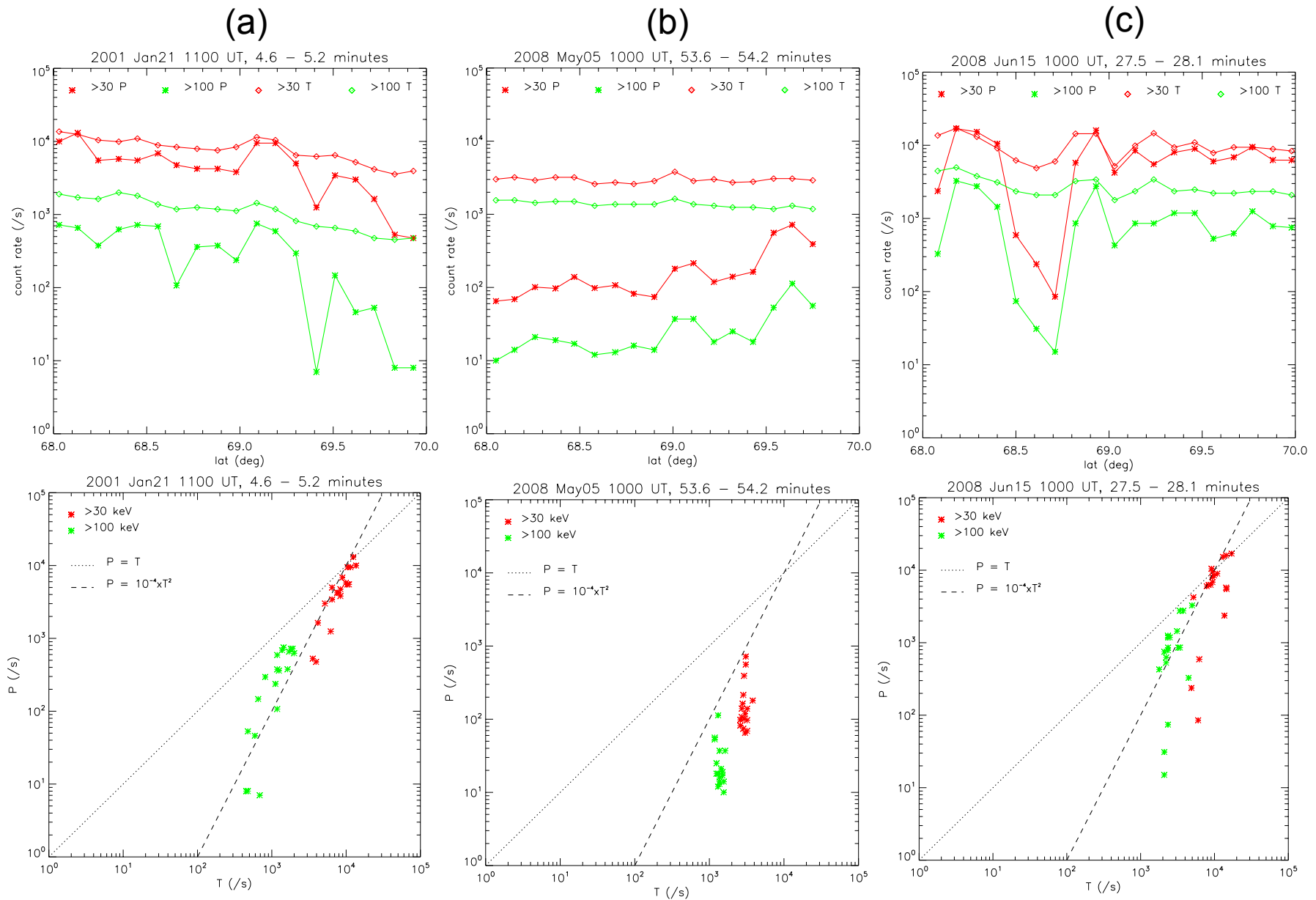
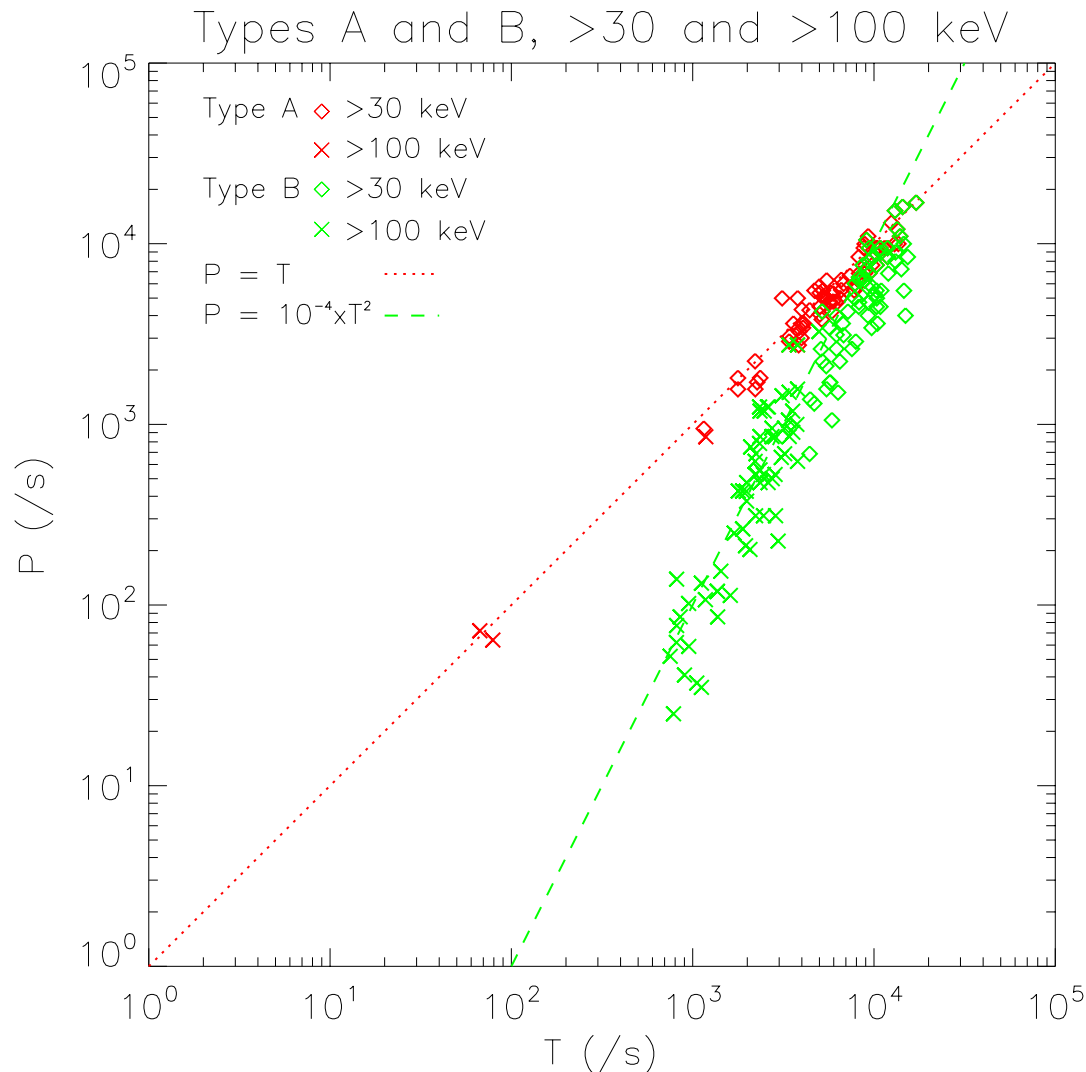


Figure 4: Examples of the three types of behaviour of P with respect to T:
(a) types A and B; (b) type C; (c) types A, B and C.

Type	30 keV				100 keV			
	Total		Total alone		Total		Total alone	
	No.	%	No.	%	No.	%	No.	%
A	18	42%	1	2%	2	5%	0	0%
B	19	44%	7	16%	8	19%	4	9%
C	24	56%	9	21%	23	53%	19	44%

**Table 1: Number of passes in which the three types of behaviour occur, in a sample of 43 passes.
 (“Total alone” means that this was the only type identified during the pass.)**

Some common properties (types A and B)



Type A behaviour was seen at 30 keV down to about 10^3 counts/s in T30. There were relatively few occurrences at 100 keV.

Type B behaviour was seen above about 3×10^3 in T30, and above about 10^3 in T100. Nearly all values of P are within a factor of 2 or 3 of the relation $P = 10^{-4} T^2$. The samples were from all times of year and from three years of different solar activity.

Figure 5: Variation of P with T for type A (individual points selected from 18 passes, red) , and type B (from a sample of 5 passes, green).

Some common properties (type C)

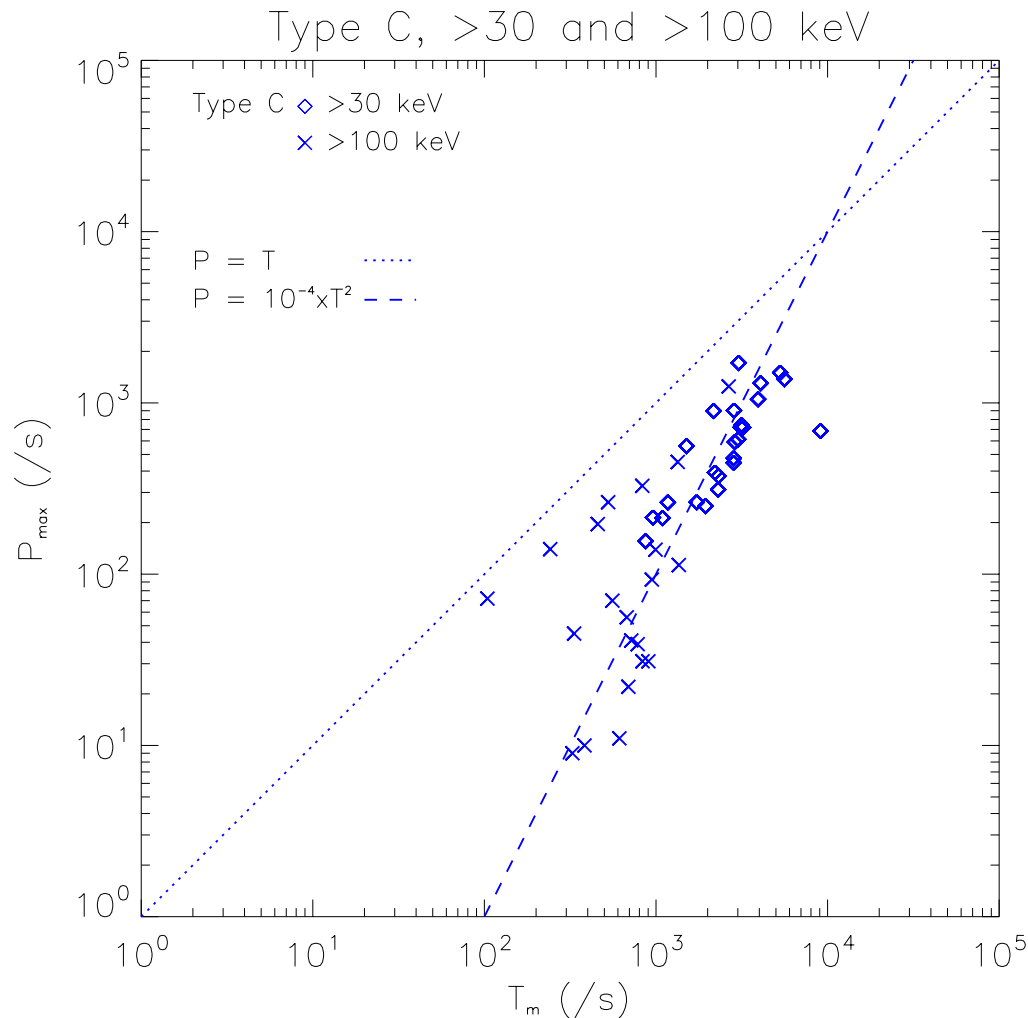


Figure 6: Variation of P with T for type C.

From clear examples of type C, in which there is a significantly large variation in P without a systematic variation in T , the largest value of P (i.e. P_{\max}) was selected for each sample.

Figure 6 plots P_{\max} against the mean value of T (i.e. T_m) for each case. It is noteworthy that these points follow virtually the same relation ($P_{\max} = 10^{-4} T_m^2$) as those in type B.

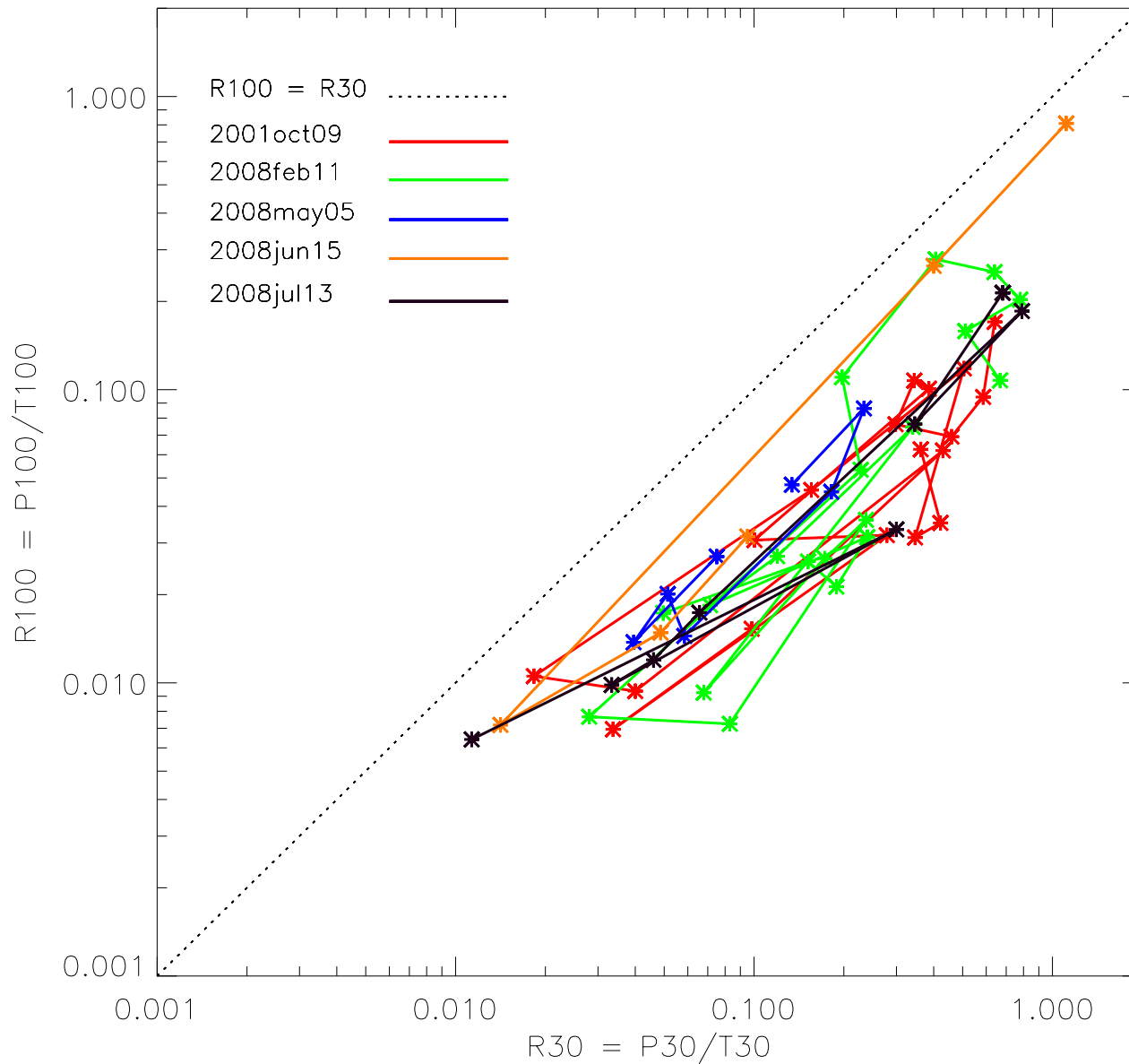
In our sample, the five 100 keV points closest to the $P=T$ line occurred when the 30 keV behaviour was of type A.

- Type A fits the concept of strong diffusion with an almost isotropic pitch angle distribution [2].
- Type B ($P \propto T^2$) is consistent with “unstable” weak diffusion [2] in which the trapped particles generate waves in proportion to their intensity, these waves then scattering some proportion of the trapped flux into the loss cone. (“Self-generated” might be a better description than “unstable”.)
- Within a single “drop” (type C) the maximum value of P also follows an essentially $P \propto T^2$ variation (Figure 6), the relationship being virtually the same ($P = 10^{-4}T^2$) at both 30 and 100 keV. The other values within the “drop” are smaller than $10^{-4}T^2$ in most cases. Moreover, the amount of reduction is proportionally the same at each energy (Figure 7).

- $P \propto T^2$ implies that the precipitated flux is always softer than the trapped –

$$\frac{P_{100}/P_{30}}{T_{100}/T_{30}} = \frac{T_{100}}{T_{30}} < 1$$

- There is no variation of hardness during a single drop $\left(\frac{P_{100}}{T_{100}} \propto \frac{P_{30}}{T_{30}} \right)$



- Examples of type 3 behaviour from five passes.
- The variation of R100 with R30 is essentially linear.

Figure 7: Type 3 “drops”, R100 against R30

Conclusions

- From a study of the POES passes over a high-latitude site, using 2s data on >30 and >100 keV electrons, three types of behaviour have been identified.
- At the highest fluxes the precipitated component (P) tends to vary in proportion to the trapped (T), but over most of the range below about $T = 5 \times 10^3$ (counts/s) a square-law relationship ($P \approx 10^{-4}T^2$) is most dominant.
- These types of behaviour seem consistent with scattering by self-generated waves as in the classical theory (e.g. [2]).
- However, about half the passes include instances in which the precipitated flux varies over a considerable range (at least a factor of 10) while the trapped component hardly changes. Some additional mechanism is required to explain this behaviour.

Acknowledgement

We thank Dr. D. S. Evans for providing the POES data and advising on its use.

References

1. Hargreaves, J.K., Birch, M.J., Evans, D.S., “On the fine structure of medium energy electron fluxes in the auroral zone, and related effects in the ionospheric D-region”, *Annales Geophysicae*, 28, 1107–1120, 2010.
2. Thorne, R.M., “The importance of wave-particle interactions in the magnetosphere”. *Critical problems of magnetospheric physics. Proc. Joint COSPAR/IAGA/URSI Symposium, Madrid, 211-225. Published by National Academy of Sciences, Washington DC, 1972.*